



Comparison of dragonfly algorithm and Harris hawks optimization evolutionary data mining techniques for the assessment of bearing capacity of footings over two-layer foundation soils

Hossein Moayed^{1,2} · Mu'azu Mohammed Abdullahi³ · Hoang Nguyen⁴ · Ahmad Safuan A. Rashid⁵

Received: 10 July 2019 / Accepted: 26 July 2019 / Published online: 2 August 2019
© Springer-Verlag London Ltd., part of Springer Nature 2019

Abstract

By assist of novel evolutionary science, the classification accuracy of neural computing is improved in analyzing the bearing capacity of footings over two-layer foundation soils. To this end, Harris hawks optimization (HHO) and dragonfly algorithm (DA) are applied to a multi-layer perceptron (MLP) predictive tool for adjusting the connecting weights and biases in predicting the failure probability using seven settlement key factors, namely unit weight, friction angle, elastic modulus, dilation angle, Poisson's ratio, applied stress, and setback distance. As the first result, incorporating both HHO and DA metaheuristic algorithms resulted in higher efficiency of the MLP. Moreover, referring to the calculated area under the receiving operating characteristic curve (AUC), as well as the calculated mean square error, the DA-MLP (AUC = 0.942 and MSE = 0.1171) outperforms the HHO-MLP (AUC = 0.915 and MSE = 0.1350) and typical MLP (AUC = 0.890 and MSE = 0.1416). Furthermore, the DA surpassed the HHO in terms of time-effectiveness.

Keywords Bearing capacity analysis · Dragonfly algorithm · Evolutionary science

1 Introduction

Ultimate bearing capacity has been defined as the value of maximum pressure that soil can support without occurring failure [1, 2]. Currently, the influences of the ultimate bearing capacity in the case of shallow strip footings have been highly considered by scholars in the field of geotechnical engineering design as a major issue. It is called a major problem, because

is considered as the interface among soil and upper structures. There are different analytical procedures that are according to limit equilibrium theory [3]. In the literature, there are various solutions that can be widely used to predict and measure the bearing capacity parameter. In previous attempts, different analytical and experimental methods, including limit analysis [4], experimental methods [5], analytical methods [6], limit equilibrium [7], and numerical methods [8] have been proposed in the case of the footings' bearing capacity set on the slope crest.

Natural soils that are deposited in layers of homogeneous soil are rarely discovered. The ultimate bearing capacity in the case of the multi-layer soil is not commonly treated such as a single layer of soil, since, for each layer, the soil stiffness and stability factors are distinct. Many scholars have focused on theories related to the bearing capacity for multi-layered soil. In this way, two cases which may be deemed as inhomogeneous sands layer are: (1) stronger soil that placed onto a layer of weaker soil and (2) weaker sand that placed onto a layer of solid soil [9]. The usual computational approaches commonly consider designing the ultimate bearing capacity or q_{ult} by Eqs. 1 and 2 that are suggested in Refs. [3, 10]:

$$q_{ult-Terzaghi(1943)} = c'N_c + qN_q + \frac{1}{2}\gamma BN_\gamma \quad (1)$$

✉ Hossein Moayed
hossein.moayed@tdtu.edu.vn

¹ Department for Management of Science and Technology Development, Ton Duc Thang University, Ho Chi Minh City, Vietnam

² Faculty of Civil Engineering, Ton Duc Thang University, Ho Chi Minh City, Vietnam

³ Civil Engineering Department, University of Hafr Al-Batin, Hafr Al-Batin, Eastern Province 39524, Kingdom of Saudi Arabia

⁴ Institute of Research and Development, Duy Tan University, Da Nang 550000, Vietnam

⁵ Centre of Tropical Geoenvironment (Geotropik), School of Civil Engineering, Faculty of Engineering, Universiti Teknologi Malaysia, Johor Bahru, Malaysia

$$q_{\text{ult-Hasen(1970)}} = c'N_c d_c S_c + q'N_q d_q S_q + \frac{1}{2}\gamma B N_\gamma d_\gamma S_\gamma. \quad (2)$$

In above relations, N_c , N_q , and N_γ stand for the parameters of the bearing capacity that are based on the overburden pressure (q), the internal friction angle (φ), footing width (B), cohesion (c'), and soil unit weight (γ).

Recently, various data mining models like artificial neural network (ANN) and fuzzy systems have been promisingly used to deal with geotechnical issue including bearing capacity [11–15]. In this regards, Maizir et al. [16] explained approaches of the finite element and also ANN for predicting the pile bearing capacity in the case of sandy soil. They used ANN models to predict the bearing capacity utilizing dynamic load test information, and compared the results of a finite-element approach with an empirical method. They found that finite-element and ANNs' approaches have almost the same results for the ultimate load. In addition, they showed that axial bearing capacity of piles is entirely changeable. Likewise, Ziaee et al. [17] suggested a novel design equation about predicting the bearing capacity of shallow structures on rock masses by taking into account ANN model. They simulated the bearing capacity with considering internal friction angle about the rock mass, joint spacing ratio for basis width, rate of rock mass, and unindicated compressive rock strength. Moreover, they used general data sets of plate load, rock socket, footing load test in the large-scaled state, and centrifuge rock socket outcomes for expanding the model. The results of their research proved an appropriate efficiency of the derivative model to predict the bearing capacity of shallow bases. The suggested estimating relation is considerably more efficient compared to traditional relations. Lee and Lee [18] used error back propagation neural networks for estimating the ultimate bearing capacity about piles. They verified the applicability of the ANNs with outcomes of model pile load measurements and showed that the maximum difference between experimental and prediction data is around 25%. Moayedi and Hayati [19] showed the outcomes of various non-linear machine learning as well as soft computing-based algorithm [e.g., radial basis neural network (RBNN), support vector machine (SVM), regression fitting model (TREE), etc.]. They evaluated them by taking into account different statistical indices. After performing this task, the most precise algorithm was suggested for estimating the solution. They have also compared the estimated data with the FEM data and showed good validity for FFNN solutions.

Moreover, many scholars have employed evolutionary knowledge for enhancing the results of regular predictive models in many engineering problems [20–26]. Moayedi et al. [27] used different evolutionary algorithms such as differential evolution (DE) and genetic algorithm along with particle swarm optimization for optimizing machine learning models

to estimate the ultimate bearing capacity in the case of shallow footing on multi-layered soil state. They stated that all optimized methods have a promising performance. However, the algorithm of PSO–ANN showed better performance than other methods. Likewise, Moayedi and Armaghani [28] have suggested and evaluated an ANN optimized with imperialism competitive algorithm (ICA) approach to predict the bearing capacity about driven pile into cohesionless soil. By means of various accuracy criteria and high validity, the expanded ICA-ANN algorithm was deduced, and they suggested it as a novel model about deep foundation engineering.

Although famous optimization techniques (e.g., PSO, ICA, GA, etc.) have been widely used to solve the problem of bearing capacity, utilizing and evaluating more-state-of-the-art colleague algorithms are considered as a gap of knowledge in this field. Hence, the pivotal objective of the current effort lies in presenting and evaluating two novel state-of-the-art hybrid techniques, namely Harris hawks optimization (HHO) and dragonfly algorithm (DA) for investigating the bearing capacity in the position of a classification issue. Notably, the literature survey (to the best knowledge of the authors) indicates that our proposed algorithms have not been previously used in the same field of study. Meanwhile, receiving operating characteristic (ROC) diagram is used to evaluate the classification accuracy of the models.

2 Methodology

2.1 Artificial neural network

Mimicking the interactions between the neurons in the biological neural network, the basic theory of artificial neural network (ANN) was first discussed by McCulloch and Pitts [29]. The most outstanding merit of this method is its capability for mapping the non-linear interactions between some dependent and independent parameters ASCE Task Committee [30]. Figure 1 shows a general structure of a widely used type of ANNs, namely multi-layer perceptron (MLP).

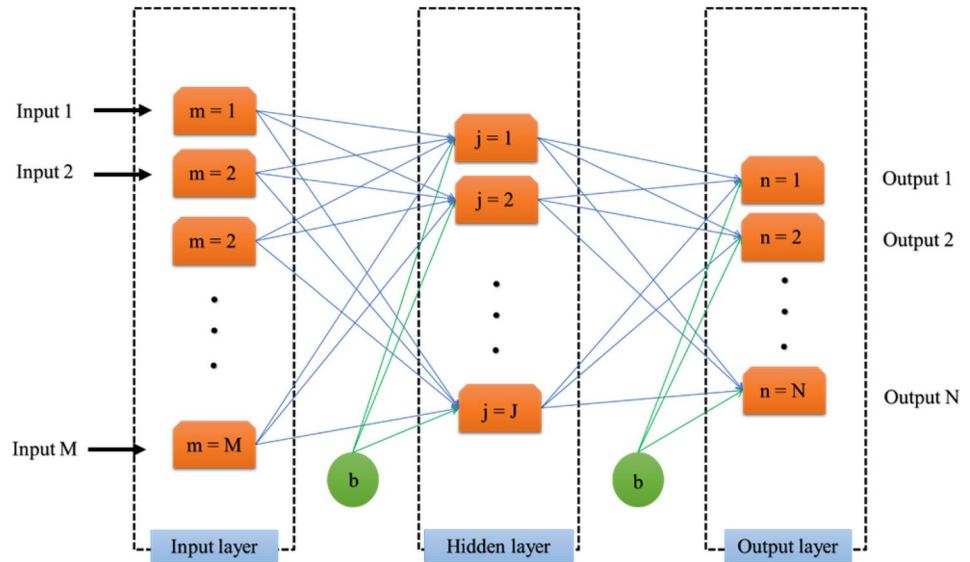
In general, the MLP uses Levenberg–Marquardt (LM) [31, 32], which is a powerful approximation to Newton's method [33]. In comparison with conventional gradient descent (GD) technique, the LM has shown higher robustness [34, 35]. More specifically, it aims to minimize the sum of squares function ($V(x)$) as follows:

$$V(x) = \sum_{i=1}^N e_i^2(x) \quad (3)$$

$$\Delta \underline{x} = - \left[\nabla^2 V(x) \right]^{-1} \nabla V(x). \quad (4)$$

In the above relations, $\nabla^2 V(x)$ and $\nabla V(x)$ are the Hessian and gradient matrixes, respectively.

Fig. 1 The structure of an MLP neural network



Next, assuming $J(x)$ as the Jacobean matrix, then we have the following:

$$\begin{aligned} \nabla V(x) &= J(x)e(x) \\ \nabla^2 V(x) &= J^T(x)J(x) + S(x), \\ S(x) &= \sum_{i=1}^N e_i \nabla^2 e_i(x). \end{aligned} \tag{5}$$

When $S(x) \approx 0$, Eq. 4 can be expressed as follows:

$$\Delta x = [J^T(x)J(x)]^{-1} J^T(x)e(x). \tag{6}$$

Finally, let λ determine the behavior of the algorithm, then the LM is expressed as follows:

$$\Delta x = [J^T(x)J(x) + \lambda I]^{-1} J^T(x)e(x). \tag{7}$$

2.2 Harris hawks optimization

The name Harris hawks optimization (HHO) implies a recently developed optimization technique suggested by Heidari et al. [36]. This algorithm mimics the cooperative behavior of Harris’ hawks to address various optimization problems. By performing a good teamwork, the hawks aim to hunt the prey in some steps including tracing, encircling, approaching, and finally attacking. These hawks do a co-called maneuvering “surprise pounce” for catching an escaping hunt. As shown in Fig. 2, two main phases of the HHO

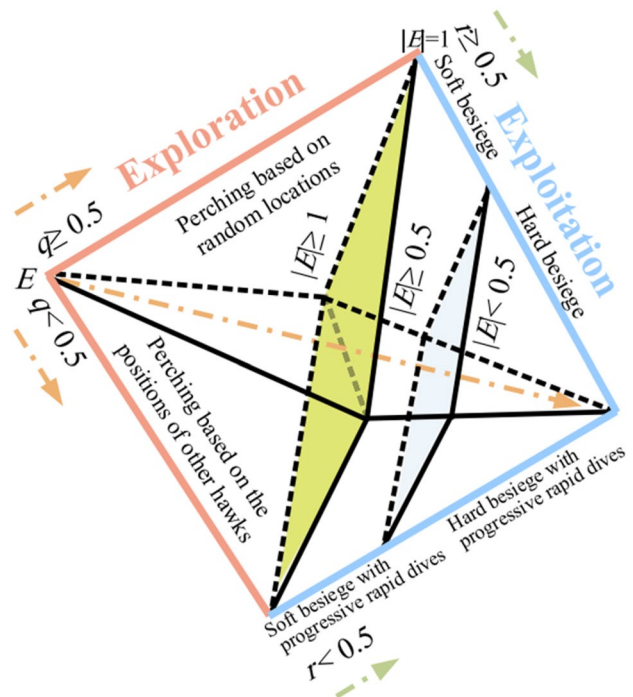


Fig. 2 Different phases of Harris hawks optimization (after Heidari et al. [36])

are exploration and exploitation, where a middle phase is defined for transferring between them.

The first phase comprises waiting, seeking, and discovering the proposed prey. Let X_{rabbit} stand for the rabbit position, and then, the position of the hawks is defined as follows:

$$X(\text{iter} + 1) = \begin{cases} X_{\text{rand}}(\text{iter}) - r_1 |X_{\text{rand}}(\text{iter}) - 2r_2 X(\text{iter}) & \text{if } q \geq 0.5 \\ (X_{\text{rabbit}}(\text{iter}) - X_m(\text{iter})) - r_3 (LB + r_4 (UB - LB)) & \text{if } q < 0.5 \end{cases} \tag{8}$$

where X_{rand} is one of the existing hawks which is proposed randomly. Moreover, r_i ($i = 1, 2, 3, 4, q$) is a random number which ranges in $[0, 1]$. In addition, X_m denotes the average position. Considering X_i and N as the place of the hawks and their size, respectively, X_m is calculated by the following equation:

$$X_m(iter) = \frac{1}{N} \sum_{i=1}^N X_i(iter). \tag{9}$$

At the second stage, let T and $E_0 \in (-1.1)$ be the maximum size about the repetitions and the initial energy, the escaping energy of the hunt (E), which can change the exploration and exploitation, is formulated as follows:

$$E = 2E_0 \left(1 - \frac{iter}{T} \right). \tag{10}$$

In this part, based on the magnitude of $|E|$, it is decided to start the exploration phase ($|E| \geq 1$) or exploiting the neighborhood of the solutions ($|E| < 1$).

In the last phase, regarding the value of $|E|$, the hawks decide to apply a soft ($|E| \geq 0.5$) or hard besiege ($|E| < 0.5$)

to catch it from several directions. Remarkably, the escaping probability of the target is calculated by the parameter r , so that if it is larger than 0.5, the hunt successfully escapes and vice versa [37].

2.3 Dragonfly algorithm

Inspired by migration (dynamic swarm) and hunting (static swarm) behavior of Dragonfly herds, Mirjalili [38] proposed Dragonfly algorithm (DA) for the first time. It has shown a high capability for optimizing various engineering problems [39–41]. The Dragonflies’ life has two stages. The first stage, called nymph, is longer and the second stage is known as puberty. The hunting operation gets started by making some small groups for investigating a small region. And they change their position suddenly for hunting small insects. This is while they construct large groups during the migration [42]. As Fig. 3 illustrates, this algorithm draws on five stages of separation, alignment, cohesion, attracting to prey, and distraction from the enemy.

Mathematically, the values belonging to the separation, alignment, cohesion, attraction to food, and confusion of

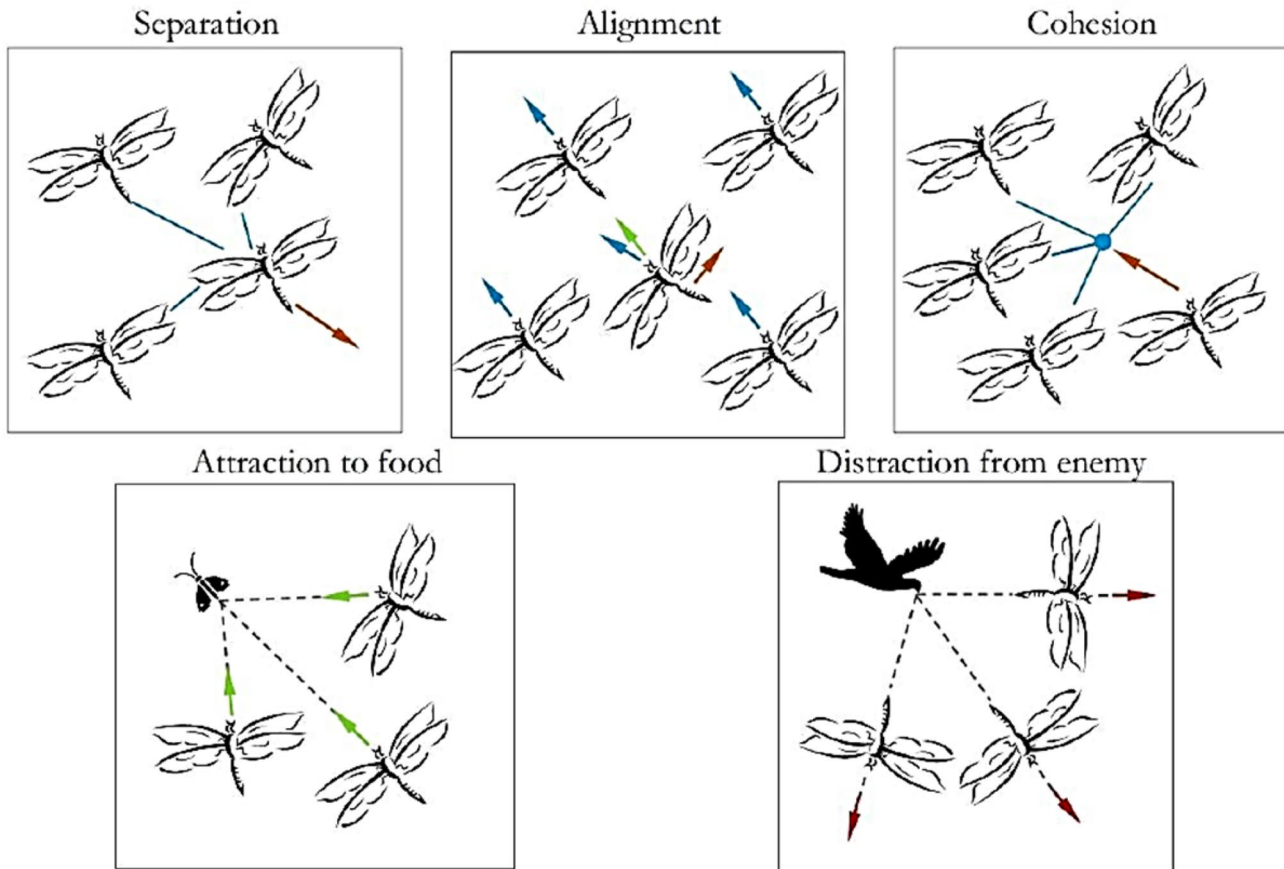


Fig. 3 Different phases of the DA algorithm (after Mirjalili [38])

enemy actions are computed by Eqs. 11, 12, 13, 14, and 15, respectively:

$$S_i = - \sum_{j=0}^n X - X_j \tag{11}$$

$$A_i = - \frac{\sum_{j=0}^n V_j}{n} \tag{12}$$

$$C_i = - \frac{\sum_{j=0}^n X_j}{n} - X \tag{13}$$

$$F_i = X^f - X \tag{14}$$

$$E_i = X^e - X, \tag{15}$$

in which X , X^f , and X^e stand for the positions of the proposed dragonfly, the food source, and the enemy, respectively. Moreover, V_j denotes the j th dragonfly velocity, and also n shows and the number of involved members.

Furthermore, assuming a , s , e , f , c , e , and w as the weights pertaining to related element, Eqs. 16 and 17 are used to update the dragonflies’ position for trying different weight solutions [38]:

$$\Delta X_{i,j} = (sS_j + aA_j + cC_j + fF_j + eE_j) + w\Delta X_{i-1,j-1} \tag{16}$$

$$X_{i,j} = X_{i-1,j-1} + \Delta X_{i,j}. \tag{17}$$

The terms e and w in above relations can be calculated by Eqs. 18 and 19. Note that, in exploration (i.e., the dynamic phase), the alignment values of dragonflies are aimed to be larger than cohesion values. Aversely, the cohesion values are projected to be larger in exploitation (i.e., the static phase) to have the capability of attacking.

$$e = 0 \cdot 1 - i * \left(\frac{0 \cdot 1}{\frac{I}{2}} \right) \tag{18}$$

$$w = 0 \cdot 9 - i * \left(\frac{0 \cdot 9 - 0 \cdot 4}{I} \right), \tag{19}$$

where a , s , and c symbolize random numbers in the extent $[0 - 2e]$, i is the going repetition, and f shows a random number in the extent $[0 - 2]$. Also, the term I denotes the number of repetitions [43, 44].

3 Data collection

T data set which was used to train the intelligent models of this research was the outcome of an extensive finite-element modeling, investigating a shallow footing in 2D

axisymmetric conditions. The proposed footing was analyzed on a two-layered soil. This is worth noting that both members of the designed system (i.e., the footing and soil) are analyzed by 15-node triangular elements. Besides, the Mohr–Coulomb is considered for the material model. A total of 901 stages were implemented by considering seven effective factors including unit weight (kN/m^3), friction angle, elastic modulus (kN/m^2), dilation angle, Poisson’s ratio (ν), applied stress (kN/m), and setback distance (m), where the settlement (m) is extracted as the output. The values of the settlement ranged in $[0 - 0.10 \text{ m}]$. To change the problem into the classification mode, the target data were classified into two categories: (1) the settlements below 0.05 represent the failure of the system and were presented by 1, and (2) the settlements above 0.05 represent the stability of the system and were presented by 0. In the following, similar to many previous studies [45, 46], the acquired data set was divided into the training and testing groups containing 80% (i.e., 721 rows) and 20% (i.e., 180 rows) of whole samples, respectively. Figure 4 shows the distribution of the considered key factors.

4 Results and discussion

This paper addresses two novel optimizations of ANN for analyzing the bearing capacity of a two-layered soil with different properties. The proposed optimization techniques are Harris hawks optimization and dragonfly algorithm, which were incorporated with an MLP network to find the most appropriate structure of it. To create the required data set, seven key factors of unit weight, friction angle, elastic modulus, dilation angle, Poisson’s ratio, applied stress, and setback distance were considered to implement 901 finite-element simulations for shallow footing located on double-layered soil. The settlement was then acquired as the output. Out of 9 rows, 80% (i.e., 721 samples) were randomly selected to train the proposed MLP, HHO-MLP, and DA-MLP models and the remaining 20% (i.e., 180 samples) were used to evaluate the accuracy of the predictions. In this regard, mean square error and mean absolute error were defined as follows to measure the error of the performance:

$$\text{MSE} = \frac{1}{N} \sum_{i=1}^N \left(Y_{i_{\text{observed}}} - Y_{i_{\text{predicted}}} \right)^2 \tag{20}$$

$$\text{MAE} = \frac{1}{N} \sum_{i=1}^N \left(Y_{i_{\text{observed}}} - Y_{i_{\text{predicted}}} \right), \tag{21}$$

in which $Y_{i_{\text{observed}}}$ and $Y_{i_{\text{predicted}}}$ represent the observed and predicted settlements, respectively. Also, N stands for the

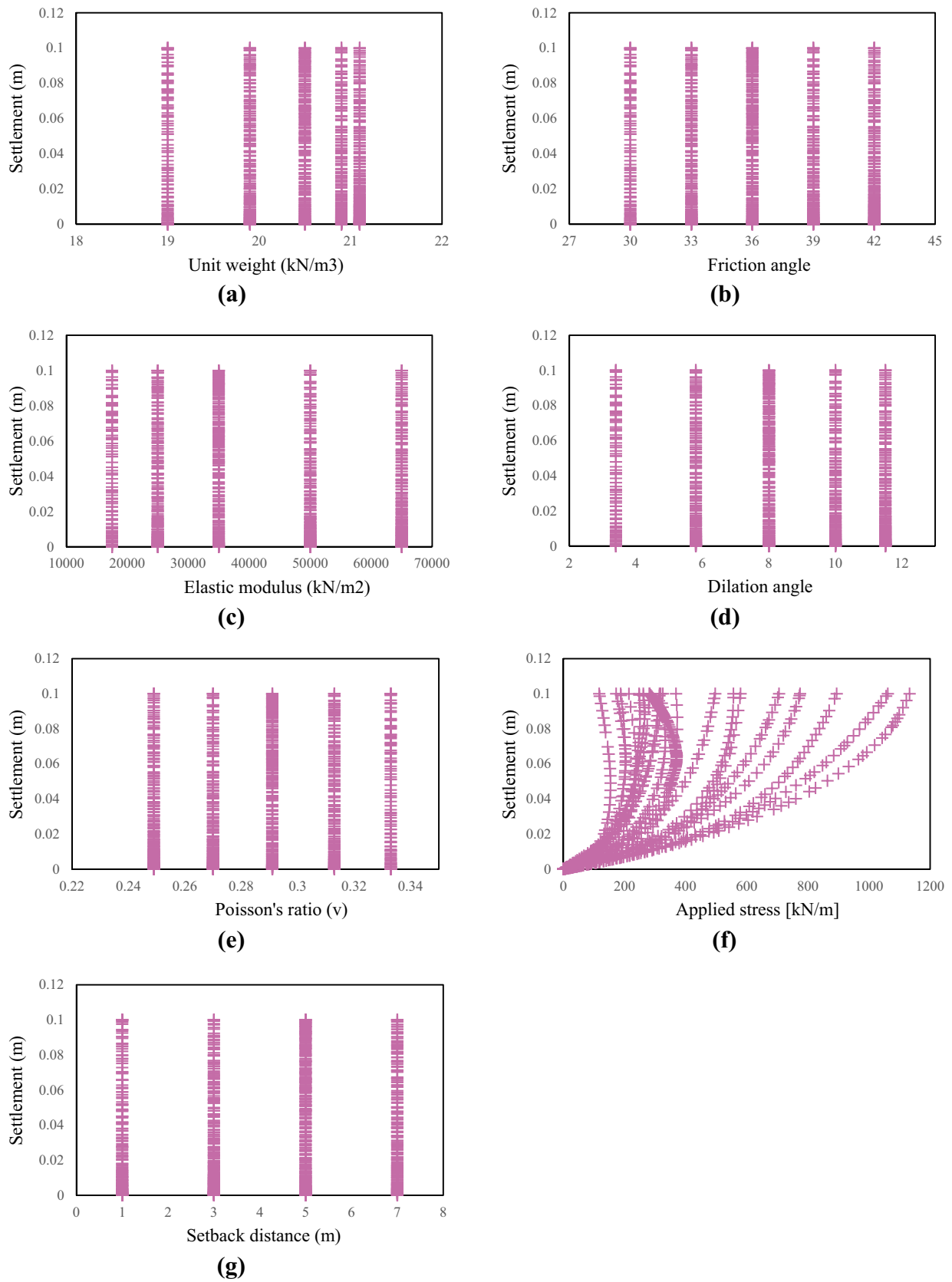


Fig. 4 Distribution of bearing capacity influential factors versus the settlement

number of samples. Moreover, the area under the receiving operating characteristic curve (AUC) criteria was used to measure the accuracy of classification. The ROC curve is a good indicator of the accuracy of natural hazard modeling [47] which plots the specificity versus the sensitivity [47–49].

4.1 Optimizing the MLP using HHO and DA conventional algorithms

The most proper structure of the models was determined by executing an extensive trial and error process. Note that all models were coded and implemented in the programming language of MATLAB. At first, it was found that the MLP with six neurons in its hidden layer presents more reliable prediction among the MLPs with the number of neurons varying from 1 to 10. Therefore, this structure was used as the basic model for the HHO-MLP and DA-MLP ensembles. Following this, the HHO and DA were applied to the MLP to find the best values for computational parameters (i.e., the connecting weights and biases). Based on the population size, ten different structures of the HHO-MLP and DA-MLP networks were tested within 1000 repetitions to achieve the best complexity of the models. In this sense, the population size varied from 10 to 100 with ten intervals. The MSE was defined as the objective function for measuring the performance error at the end of each iteration. Notably, each structure performed six times to ensure about the repeatability of them.

Figure 5a, b shows the results of the sensitivity analysis of the HHO-MLP and DA-MLP models. As is seen, the HHO keeps reducing the MSE until the last try, while the DA stops this procedure after nearly 500th iteration. According to these charts, the lowest objective function is obtained for the HHO-MLP ($MSE = 0.117559367$) and DA-MLP ($MSE = 0.097887729$) with the population sizes of 50 and 60, respectively. This is worth noting that the elite HHO took around 1662 s for optimizing the MLP, while this value was 924 s for the DA.

4.2 Accuracy assessment of the MLP, HHO-MLP, and DA-MLP predictive models

In this section, the performance of the used predictive models is evaluated in both training and testing stages by means of three well-known accuracy indices of MSE, MAE, and AUC. Figure 6 illustrates the results. In this figure, the observed classification values (i.e., 0 and 1) are graphically compared with the estimated values. In addition, the error (i.e., the difference between the observed and predicted classification values) is depicted alongside the histogram of the errors. Based on the results, the training outputs of the MLP, HHO-MLP, and DA-MLP range in $[-0.2689$ to $1.0562]$,

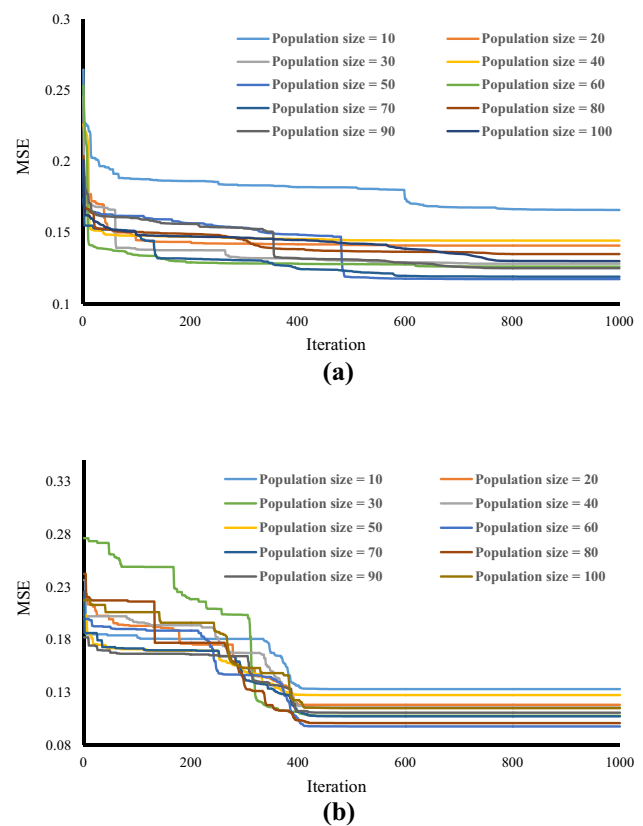


Fig. 5 Executed sensitivity analysis based on the population size

$[-0.3487$ to $1.0947]$, and $[-0.1778$ to $1.0862]$, respectively. As for the testing results, these extents were $[-0.2341$ to $1.0724]$, $[-0.3367$ to $1.1137]$, and $[-0.1629$ to $1.0852]$. According to Fig. 6, the prediction results of the reinforced MLPs have more consistency with the targets, compared to the typical MLP. It shows the efficiency of the applied HHO and DA evolutionary algorithms. In the following, the results are evaluated more accurately.

After drawing the ROC curves related to the training and testing results, the area under those curves is calculated to indicate the classification accuracy. The obtained AUCs, as well as the calculated MSEs and MAEs, are presented in Table 1 to develop a ranking system. In this system, a ranking score is assigned to each model based on the obtained criteria. Finally, the total ranking score (TRS) (i.e., the summation of the training and testing scores) determines the most successful model.

As the table denotes, in the training phase, the MSE error criterion decreased from 0.1283 to 0.1175 (i.e., by 8.42%) and 0.0978 (i.e., by 23.77%), respectively, by applying the HHO and DA algorithms. Likewise, the MAE was reduced from 0.3045 to 0.2927 (i.e., by 3.88%) and 0.2605 (i.e., by 14.45%). Also, these algorithms helped the MLP to increase the classification accuracy from 91.6 to 94.4% and 96.8%.

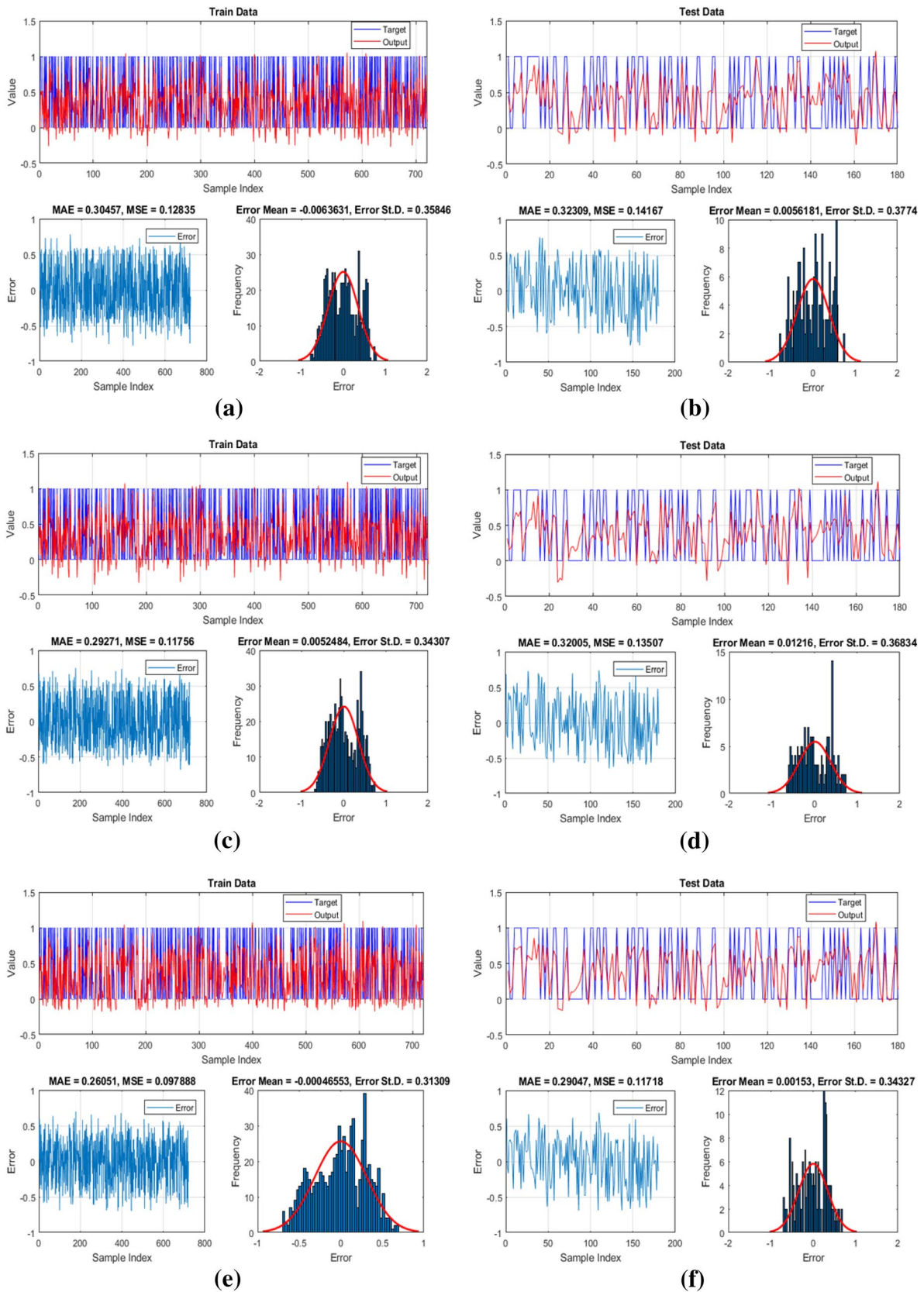


Fig. 6 The results obtained for **a, b** MLP, **c, d** HHO-MLP, and **e, f** DA-MLP predictions, respectively, for the training and testing samples

Table 1 The developed ranking system based on obtained accuracy criteria

Ensemble models	Network results						Ranking score						Total ranking score (TRS)	Rank
	Training phase			Testing phase			Training phase			Testing phase				
	MSE	MAE	AUROC	MSE	MAE	AUROC	MSE	MAE	AUROC	MSE	MAE	AUROC		
MLP	0.1283	0.3045	0.916	0.1416	0.3230	0.890	1	1	1	1	1	1	6	3
HHO-MLP	0.1175	0.2927	0.944	0.1350	0.3200	0.915	2	2	2	2	2	2	12	2
DA-MLP	0.0978	0.2605	0.968	0.1171	0.2904	0.942	3	3	3	3	3	3	18	1

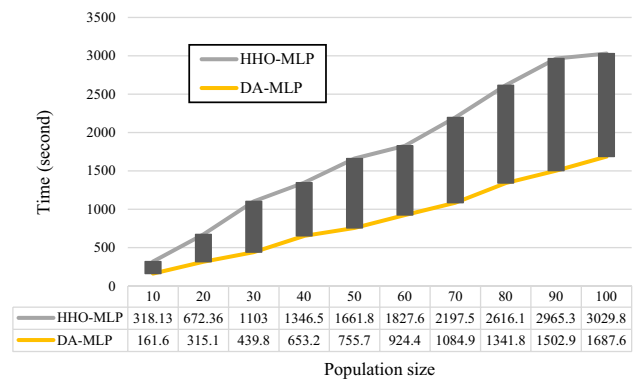


Fig. 7 The performance time of the used HHO-MLP and DA-MLP

As for the testing phase, the MSE fell from 0.1416 to 0.1350 (i.e., by 4.66%) and 0.1171 (i.e., by 17.30%). The decrease of the testing MAE from 0.3230 to 0.3200 (i.e., by 0.93%) and 0.2904 (i.e., by 10.09%) is another evidence for the effectiveness of the applied algorithms in improving the applicability of the MLP. Besides, the generalization accuracy of the MLP rose from 89.0 to 91.5% and 94.2%.

All in all, according to the results of the developed ranking system, the DA-based ensemble (TRS = 18) outperformed two other models in terms of all three MSE, MAE, and AUC, in both training and testing phases. After that, the HHO-based ensemble (TRS = 12) presented a more reliable approximation than the unreinforced MLP (TRS = 6).

A remarkable point is the time-effectiveness of the applied metaheuristic algorithms. Figure 7 compares the calculation time of the optimized HHO and DA algorithms within 1000 repetitions. As explained previously, the DA has a faster convergence as it reaches the lowest error with nearly 500 tries. This is while the HHO continues decreasing the error until the end. Therefore, it can be deduced that these algorithms minimized the objective function in approximately 1662 (HHO with population size = 50 and the number of iterations = 1000) and 460 s (DA with population size = 60 and the number of iterations = 500). Hence, in addition to the accuracy, the DA is also more effective in terms of the calculation time.

5 Conclusions

Having a reliable approximation of bearing capacity is a fundamental task in geotechnical engineering. Due to the complexity of such problems, many scholars have employed hybrid evolutionary algorithms for dealing with them. The pivotal aim of this research was to investigate the potential of Harris hawks optimization and dragonfly algorithm in optimizing the performance of artificial neural network applied for stability analysis of a two-layered soil. The results of

the executed sensitivity analysis showed that the HHO and DA with the population sizes of 50 and 60 performed better than other structures. Also, the calculated accuracy criteria revealed that both HHO and DA were successful and can be promisingly used for optimizing the weights and biases of the MLP. From comparison viewpoint, it was deduced that the outputs of the DA-MLP are in better consistency with the desired classification values. Finally, the authors believe that comparing the efficiency of the DA algorithm with other existing optimization approaches is a good idea for future works.

Compliance with ethical standards

Conflict of interest The authors declare that they have no conflict of interests.

References

- Banimahd M, Woodward P (2006) Load-displacement and bearing capacity of foundations on granular soils using a multi-surface kinematic constitutive soil model. *Int J Numer Anal Methods Geomech* 30:865–886
- Kaya A, Bulut F, Dağ S (2018) Bearing capacity and slope stability assessment of rock masses at the Subasi viaduct site, NE, Turkey. *Arab J Geosci* 11:162
- Terzaghi K, Peck RB, Mesri G (1996) *Soil mechanics in engineering practice*. Wiley, New York
- Keskin MS, Laman M (2013) Model studies of bearing capacity of strip footing on sand slope. *KSCE J Civ Eng* 17:699–711
- Zdravković L, Potts D, Jackson C (2003) Numerical study of the effect of preloading on undrained bearing capacity. *Int J Geomech* 3:1–10
- Serrano A, Olalla C, Jimenez R (2015) Analytical bearing capacity of strip footings in weightless materials with power-law failure criteria. *J Int J Geomech* 16:04015010
- Cascone E, Casablanca O (2016) Static and seismic bearing capacity of shallow strip footings. *J Soil Dyn Earthq Eng* 84:204–223
- Baazouzi M, Benmeddour D, Mabrouki A, Mellas M (2016) 2D numerical analysis of shallow foundation rested near slope under inclined loading. *Procedia Eng* 143:623–634
- Mosallanezhad M, Moayedi H (2017) Comparison analysis of bearing capacity approaches for the strip footing on layered soils. *Arab J Sci Eng* 42:3711–3722
- Bowles JE (1996) *Foundation analysis and design*. McGraw-Hill, Chicago
- Behera RN, Patra CR, Sivakugan N, Das BM (2013) Prediction of ultimate bearing capacity of eccentrically inclined loaded strip footing by ANN, part I. *Int J Geotech Eng* 7:36–44
- Bagińska M, Srokosz PE (2019) The optimal ANN Model for predicting bearing capacity of shallow foundations trained on scarce data. *KSCE J Civ Eng* 23:130–137
- Acharyya R, Dey A, Kumar B (2018) Finite element and ANN-based prediction of bearing capacity of square footing resting on the crest of $c-\phi$ soil slope. *Int J Geotech Eng* 13:1–12. <https://doi.org/10.1080/19386362.2018.1435022>
- Padmini D, Ilamparuthi K, Sudheer K (2008) Ultimate bearing capacity prediction of shallow foundations on cohesionless soils using neurofuzzy models. *Comput Geotech* 35:33–46
- Das M, Dey AK (2018) Determination of bearing capacity of stone column with application of neuro-fuzzy system. *KSCE J Civ Eng* 22:1677–1683
- Maizir H, Suryanita R, Jingga H (2016) Estimation of pile bearing capacity of single driven pile in sandy soil using finite element and artificial neural network methods. *J Int J Appl Phys Sci* 2:45–50
- Ziaee SA, Sadrossadat E, Alavi AH, Mohammadzadeh Shadmehri D (2015) Explicit formulation of bearing capacity of shallow foundations on rock masses using artificial neural networks: application and supplementary studies. *Environ Earth Sci* 73:3417–3431
- Lee I-M, Lee J-H (1996) Prediction of pile bearing capacity using artificial neural networks. *Comput Geotech* 18:189–200
- Moayedi H, Hayati S (2018) Modelling and optimization of ultimate bearing capacity of strip footing near a slope by soft computing methods. *Appl Soft Comput* 66:208–219
- Gao W, Dimitrov D, Abdo H (2018) Tight independent set neighborhood union condition for fractional critical deleted graphs and ID deleted graphs. *Discrete Contin Dyn Syst Ser S* 12:711–721
- Nguyen H, Mehrabi M, Kalantar B, Moayedi H, MaM Abdullahi (2019) Potential of hybrid evolutionary approaches for assessment of geo-hazard landslide susceptibility mapping. *Geomat Nat Hazards Risk* 10:1667–1693
- Gao W, Guirao JLG, Basavanagoud B, Wu J (2018) Partial multi-dividing ontology learning algorithm. *Inf Sci* 467:35–58
- Moayedi H, Raftari M, Sharifi A, Jusoh WAW, Rashid ASA (2019) Optimization of ANFIS with GA and PSO estimating α ratio in driven piles. *Eng Comput* 35:1–12
- Gao W, Wang W, Dimitrov D, Wang Y (2018) Nano properties analysis via fourth multiplicative ABC indicator calculating. *Arab J Chem* 11:793–801
- Gao W, Wu H, Siddiqui MK, Baig AQ (2018) Study of biological networks using graph theory. *Saudi J Biol Sci* 25:1212–1219
- Gao W, Guirao JLG, Abdel-Aty M, Xi W (2019) An independent set degree condition for fractional critical deleted graphs. *Discrete Contin Dyn Syst Ser S* 12:877–886
- Moayedi H, Moatamediyan A, Nguyen H, Bui X-N, Bui DT, Rashid ASA (2019) Prediction of ultimate bearing capacity through various novel evolutionary and neural network models. *Eng Comput* 35:1–17
- Moayedi H, Armaghani DJ (2018) Optimizing an ANN model with ICA for estimating bearing capacity of driven pile in cohesionless soil. *Eng Comput* 34:347–356
- McCulloch WS, Pitts W (1943) A logical calculus of the ideas immanent in nervous activity. *Bull Math Biophys* 5:115–133
- ASCE Task Committee (2000) *Artificial neural networks in hydrology. II: hydrologic applications*. *J Hydrol Eng* 5:124–137
- Yu H, Wilamowski BM (2011) Levenberg–marquardt training. *Ind Electron Handb* 5:1
- Moré JJ (1978) *The Levenberg–Marquardt algorithm: implementation and theory, numerical analysis*. Springer, Berlin, pp 105–116
- Marquardt DW (1963) An algorithm for least-squares estimation of nonlinear parameters. *J Soc Ind Appl Math* 11:431–441
- El-Bakry MY (2003) Feed forward neural networks modeling for K–P interactions. *Chaos, Solitons Fractals* 18:995–1000
- Cigizoglu HK, Kişi Ö (2005) Flow prediction by three back propagation techniques using k-fold partitioning of neural network training data. *Hydrol Res* 36:49–64
- Heidari AA, Mirjalili S, Faris H, Aljarah I, Mafarja M, Chen H (2019) Harris Hawks optimization: algorithm and applications. *Fut Gen Comput Syst* 97:849–872
- Bao X, Jia H, Lang C (2019) A novel hybrid Harris hawks optimization for color image multilevel thresholding segmentation. *IEEE Access* 7:76529–76546

38. Mirjalili S (2016) Dragonfly algorithm: a new meta-heuristic optimization technique for solving single-objective, discrete, and multi-objective problems. *Neural Comput Appl* 27:1053–1073
39. Sureshkumar K, Ponnusamy V (2019) Power flow management in micro grid through renewable energy sources using a hybrid modified dragonfly algorithm with bat search algorithm. *Energy* 181:1166–1178
40. Xu L, Jia H, Lang C, Peng X, Sun K (2019) A novel method for multilevel color image segmentation based on dragonfly algorithm and differential evolution. *IEEE Access* 7:19502–19538
41. Yuan Y, Lv L, Wang X, Song X (2019) Optimization of a frame structure using the Coulomb force search strategy-based dragonfly algorithm. *Eng Optim* 51:1–17
42. Khalilpourazari S, Khalilpourazary S (2018) Optimization of time, cost and surface roughness in grinding process using a robust multi-objective dragonfly algorithm. *Neural Comput Appl* 31:1–12
43. Yaseen M, Al-Madi N, Obeid N (2018) Optimizing neural networks using dragonfly algorithm for medical prediction. In: 2018 8th international conference on computer science and information technology (CSIT)
44. Mafarja M, Heidari AA, Faris H, Mirjalili S, Aljarah I (2020) Dragonfly algorithm: theory, literature review, and application in feature selection. In: *Nature-inspired optimizers*. Springer, Berlin, pp 47–67
45. Moayedi H, Mehrabi M, Mosallanezhad M, Rashid ASA, Pradhan B (2018) Modification of landslide susceptibility mapping using optimized PSO–ANN technique. *Eng Comput* 35:967–984
46. Nguyen H, Moayedi H, Foong LK, Al Najjar HAH, Jusoh WAW, Rashid ASA, Jamali J (2019) Optimizing ANN models with PSO for predicting short building seismic response. *Eng Comput* 35:1–15
47. Beguería S (2006) Validation and evaluation of predictive models in hazard assessment and risk management. *Nat Hazards* 37:315–329
48. Swets JA (1988) Measuring the accuracy of diagnostic systems. *Science* 240:1285–1293
49. Lasko TA, Bhagwat JG, Zou KH, Ohno-Machado L (2005) The use of receiver operating characteristic curves in biomedical informatics. *J Biomed Inform* 38:404–415

Publisher's Note Springer Nature remains neutral with regard to jurisdictional claims in published maps and institutional affiliations.